JOURNAL OF SOLID STATE CHEMISTRY 31, 249–255 (1980)

Kinetic Study on the System of FeOCl and Pyridine

SHINICHI KIKKAWA

The Institute of Scientific and Industrial Research, Osaka University, Suita, Osaka 565, Japan

Received July 7, 1978; in revised form April 12, 1979

The layer compound FeOCl absorbs pyridine molecules into its interlayer regions. The kinetics of this intercalation were investigated in the temperature region from room temperature to 130°C. The reaction products had different compositions, $FeOCl(pyridine)_{1/4}$ and $FeOCl(pyridine)_{1/3}$, in the temperature regions below and above 60°C, respectively. Reaction mechanisms were explained by nucleation and diffusion processes. The nucleation processes followed different rate equations in the respective temperature regions, the first-order rate law at lower temperatures, and the two-dimensional Avrami–Erofeev equation at higher temperatures. The diffusion processes were well described by two-dimensional Jander's diffusion equation. Activation energies of all processes were about 10 kcal/mole.

Introduction

Some layer compounds such as TaS_2 absorb many kinds of organic molecules into their van der Waals interlayer gap forming new layered charge transfer complexes (*1*). A mechanism for the complete process of intercalation is thought to consist of the following elementary steps. At first host materials absorb intercalates on their crystal edges. And then the absorbed intercalates diffuse into the interlayer region forming a stable intercalation compound. Diffusion and stabilization are usually observed in other inorganic solid state reactions. But intercalation is peculiarly followed by a large expansion of the interlayer distance of the host inorganic lattice. In the case of TaS_2, the interlayer distance is 6 Å and the expansion is about 6 Å for the intercalation of pyridine (*2*). So far there are few kinetic studies of the intercalation reaction (*3, 4*). FeOCl is another layer compound and easily intercalates pyridine and some pyridine derivatives into its interlayer van der Waals gap (*5*).

Experimental

Materials. Iron oxychloride was prepared in a temperature gradient of 370°C/400°C by heating a mixture of α-Fe_2O_3 and $FeCl_3$ in a sealed Pyrex tube. The duration of this reaction was 2 days. Products deposited in a cool zone were washed with water to remove excess $FeCl_3$. The obtained FeOCl was sorted out with 100 and 200 meshes. Particle size of the sample is estimated to be between 74 and 149 μm. Pyridine was dried with sodium hydroxide.

Experimental technique and apparatus. Isothermal intercalation kinetics were determined by measuring weight gain during the reaction using a silica spring microbalance as shown in Fig. 1. A silica spring having a sensitivity of 9.62 mm/100 mg extension was used. Change in weight was determined by measuring change in the spring length with a cathetometer.

A sample of about 30 mg in silica pan was weighed and suspended from the spring. The vacuum system was evacuated for at least

0022-4596/80/020249-07$02.00/0

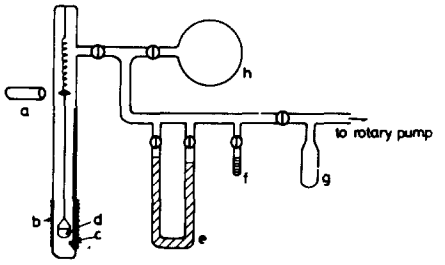

FIG. 1. Schematic representation of the intercalation reaction apparatus. a, cathetometer; b, ribbon heater; c, thermocouple; d, silica pan; e, pressure gauge; f, pyridine reservoir; g, trap; h, gas storage.

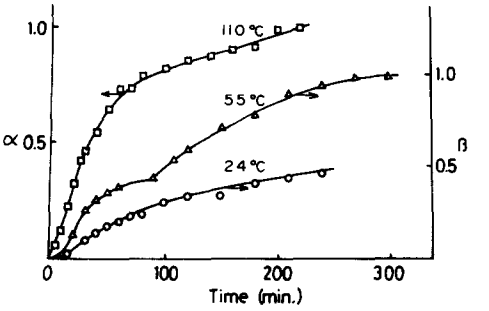

FIG. 2. Examples of isothermal weight gain at 24, 55, and 110°C. α and β are, respectively, fractional absorptions for the compositions of $FeOCl(Py)_{1/3}$ and $FeOCl(Py)_{1/4}$.

15 hr before the experiment. After the hot zone was heated to the desired temperatures, pyridine vapor was put into the system. During the experiment the vapor pressure of the whole system was kept at 12 mm Hg, a saturated vapor pressure at room temperature. Measurements were made at the following temperatures: 14, 24, 40, 55, 70, 86, 98, 110, 123, and 128°C.

Results

The compositions of the final products were determined by weight gains and chemical analyses. The products were $FeOCl(Py)_{1/3}$ and $FeOCl(Py)_{1/4}$, respectively, at high (70 ~ 128°C) and low 14 ~ 55°C) temperatures. After a reaction was completed, the reaction vessel was evacuated using a mechanical pump for about 1 hr. However, desorption of the intercalated pyridine was not detected.

Isothermal weight gain data were represented using fractional absorptions, α and β, respectively, for the final compositions of $FeOCl(Py)_{1/3}$ and $FeOCl(Py)_{1/4}$ against time. Examples are shown in Fig. 2. The absorption curves (α or β vs t) were mainly sigmoid with a short initiation period. A plateau is found around $\beta \sim 0.4$, obviously in the lower temperatures. Possible reaction processes are discussed below for the intercalation of pyridine into FeOCl.

(1) Initial stage. The results were interpreted in terms of kinetics mainly controlled by nucleation, interface reaction, or diffusion. The data were plotted using the method of Hancock and Sharp to judge which of these steps is important (*6*). As shown in Fig. 3, functions $\ln[-\ln(1-\alpha)]$ and $\ln[-\ln(1-\beta)]$ were plotted against $\ln t$, where α and β were fractional absorptions for the final products of $FeOCl(Py)_{1/3}$ and $FeOCl(Py)_{1/4}$, respectively, and t was the reaction time in minutes. The data points are almost on a straight line up to around $\alpha \sim 0.5$ and $\beta \sim 0.4$. Probable kinetic equations were derived from the gradients of these lines and tested as follows.

At temperatures higher than 70°C, the gradient is nearly 2 as shown in Fig. 3a. The method of Hancock and Sharp suggests that the rate-controlling step is a nucleation and it follows the Avrami–Erofeev equation

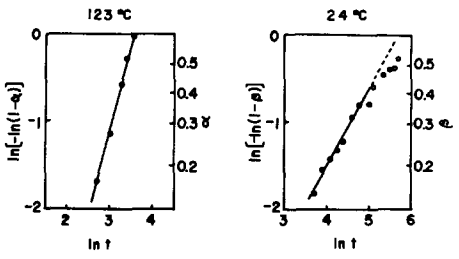

FIG. 3. Isothermal weight gain data plotted using the method of Hancock and Sharp.

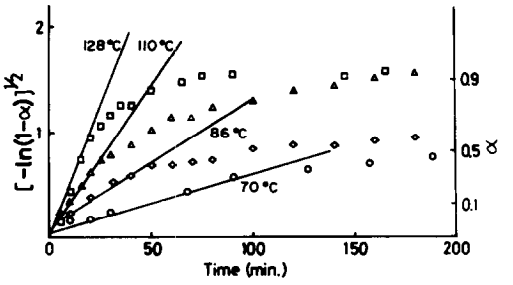

FIG. 4. Typical data plotted using the two-dimensional Avrami–Erofeev equation in the higher temperature region.

modified to the two-dimensional case, which is described below:

$$[-\ln(1-\alpha)]^{1/2} = kt.$$

Data points are on the lines, as shown in Fig. 4, in the region below $\alpha = 0.5$. Deviation from this equation is found above $\alpha = 0.5$.

At lower temperatures (below 55°C), the gradient is about 1 as seen in Fig. 3b. This gradient suggests that the rate-determining step is a two-dimensional interface reaction or a first-order nucleation. Functions of β were plotted versus t for these two processes. A better fit was obtained for the first-order nucleation process, as indicated in Fig. 5, than for the interface reaction. In this case the reaction follows the equation

$$-\ln(1-\beta) = kt.$$

This equation also fits only below $\beta = 0.4$.

(2) Diffusions step. Absorbed pyridine molecules diffuse into the inner region of FeOCl after the nucleation is completed to some extent at the crystal edges. This diffusion makes it possible for FeOCl to absorb pyridine molecules successively. Pyridine molecules drive into the very anisotropic planar spaces of the interlayer region. The famous three-dimensional Jander's diffusion controlled rate equation was modified to the two-dimensional case. As shown in Figs. 6 and 7 both α and β nicely follow the following equations:

$$[1-(1-\alpha)^{1/2}]^2 = kt,$$

$$[1-(1-\beta)^{1/2}]^2 = kt,$$

up to where α and β are about 0.8.

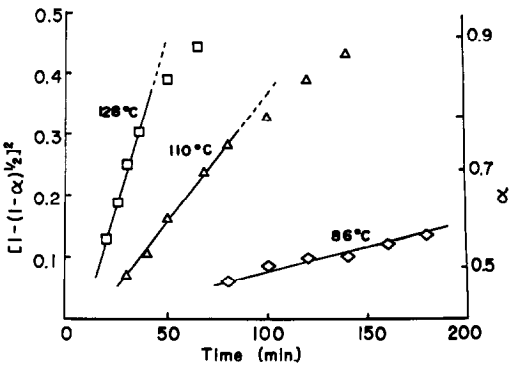

FIG. 6. Two-dimensional Jander's equation in the higher temperature region.

Discussion

A mechanism for the complete process of intercalation is thought to consist of the

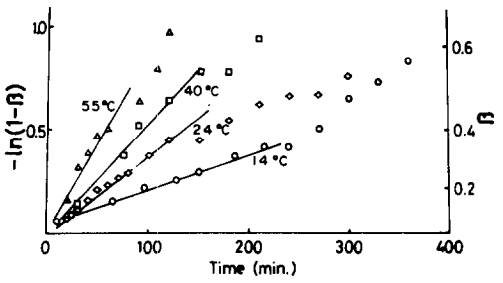

FIG. 5. Test of the first-order rate equation for typical data.

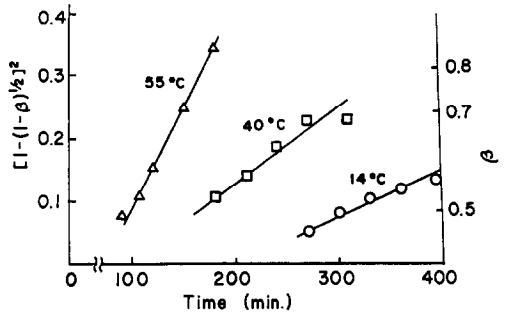

FIG. 7. Data plotted using two-dimensional Jander's equation in the lower temperature region.

following four elementary steps. Step 1, a diffusion of intercalate to the surface of the host material, is the fastest and obviously not rate determining. Step 2 is an adsorption of intercalates on the surface. It seems also unlikely that this will be the rate-determining step, because this adsorption is only physiosorption. Step 3 is a formation of the activated complex of the intercalate with the host surface atoms and a concomitant increase of the interlayer distance. It is assumed to involve chemisorption requiring energy for activation and most probably is the rate-determining step. This is confirmed by the fact that intercalation involves some types of charge transfer from the guest species to the host layers and by the experimental observation that an increase in temperature always leads to an increased rate of intercalation. Step 4 is a diffusion of the intercalate into the host lattice forming a stable intercalation compound. This step is also likely to be rate determining, especially in cases where intercalation has proceeded to a considerable extent.

Subba Rao and Shafer proposed similar mechanisms for the intercalation of metal hydroxide into TaS_2 (*3*). The reaction obeyed the first-order rate law only up to a limited reaction time t' ($t' < t_{total}$), and then for the time longer than t' it exhibited a complicated behavior with a decreasing rate due to the slow diffusion of intercalate.

In the case of FeOCl–pyridine, the intercalation is understood with a nucleation followed by a diffusion. A nucleation process is dominant in the initial stage of the reaction, then a diffusion in the following step.

Pyridine molecules are only physically adsorbed on the edges of FeOCl layers at first. Because of the basic nature of pyridine, adsorbed molecules react fairly quickly with crystal edges forming a nucleus of the intercalation compound. The interlayer distance of host layers expands only at the edges of the crystals in this stage. The inner region is not yet expanded. The expansion, however, exerts a substantial strain on the inner region of the crystal. In the lower temperature region, the reaction rate of this nucleation is given by the first-order rate equation,

$$-\ln(1-\beta) = kt,$$

as in the case of TaS_2–metal hydroxide (*3*).

The nucleation in the higher temperature region occurs much more quickly on every active site of the edges. All sites are in planes of the host layers because of the layer structure of FeOCl. The layer structure of host crystals probably affects a dimensionality of the kinetics. The nucleation process follows the two-dimensional Avrami–Erofeev equation,

$$[-\ln(1-\alpha)]^{1/2} = kt.$$

The same equation was applied to the insertions of NH_3 and ND_3 into 2H-TaS_2(*7*).

The observed rate constants at various temperatures roughly obey the Arrhenius equation in both higher and lower temperature regions as indicated in Fig. 8. The observed values of activation energies are 6 kcal/mole for the first-order rate law in a lower temperature region, and 10 kcal/mole for the Avrami nucleation rate law at higher temperatures. These values are in the range observed for chemical adsorption.

Nucleations in both temperature regions follow each above-mentioned rate law in the

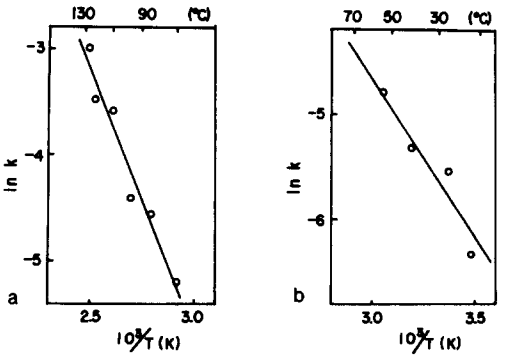

FIG. 8. Temperature dependences of rate constants k for the Avrami–Erofeev equation (a) and for the first-order rate equation (b), respectively.

initial stages of the intercalation. But deviations occur around $\alpha = 0.5$ and $\beta = 0.4$, and thereafter diffusion becomes predominant. The absorbed species at the edges diffuse into the inner region even at the beginning of intercalation. Nucleation is very fast and diffusion is sluggish in this stage. Intercalated pyridine molecules inhibit successive absorption and diffusion becomes important when some amount of pyridine is adsorbed.

A very simple model is used to understand the diffusion process. The FeOCl crystal is thought of as a disk and the intercalated pyridine molecules diffuse from the edge to the center of the disk. As illustrated in Fig. 9, the radius of the disk is r_0. According to Fick's law, the thickness of the product's layer changes, following the equation

$$\frac{d\delta}{dt} = \frac{k_1 c}{\delta},$$

where δ is the thickness of the product's layer, c is the concentration of pyridine at the edges of FeOCl, t is the time, and k_1 is a constant. Assuming that $\delta = 0$ and $t = 0$ and c is constant, this equation yields

$$\delta^2 = 2k_1 ct. \qquad (1)$$

On the other hand, the radius (r) of the unreacted part of the FeOCl disk is represented by

$$r = r_0(1-x)^{1/2},$$

where x is a fractional reaction. Then the thickness of the product's layer is given by

$$\delta = r_0 - r = r_0[1-(1-x)^{1/2}]. \qquad (2)$$

Equations (1) and (2) are combined to give

$$[1-(1-x)^{1/2}]^2 = k_2 t, \qquad (3)$$

where $k_2 = 2k_1 c/r_0^2$. As mentioned before in Figs. 6 and 7, the diffusion rate law is applicable to the intercalation of pyridine in the range where the fractional absorptions are from 0.4 to 0.8 in both the higher and lower temperature regions.

To strengthen the validity of the diffusion model, the dependences of the parameter k_2 in Eq. (3) were checked on the particle size (r_0) of FeOCl and the pyridine pressure (c). FeOCl crystals were sieved with 32, 48, 100, and 200 meshes. The particle size dependence of k_2 was examined at 110°C under the saturated pressure of pyridine. The particle sizes were 74–149, 149–297, and 297–500 μm in diameter. As shown in Fig. 10, it is expected that k_2 is proportional to $1/r_0^2$. The pressure dependence of k_2 was investigated at 110°C using the particle size of 74–149 μm. The results in Fig. 11 show that k_2 is proportional to the pyridine pressure, in other words, the concentration (c) of pyridine at edges of FeOCl.

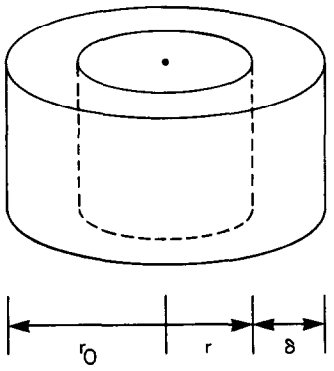

FIG. 9. Disk model of FeOCl. r_0 is the radius of the disk, r is the radius of unreacted part of FeOCl, and δ is the thickness of the product layer.

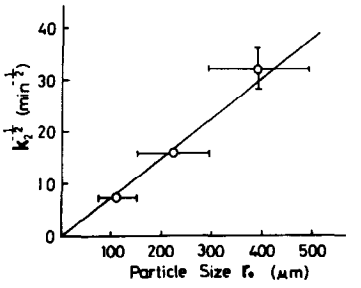

FIG. 10. Particle size dependence of rate constant k_2 of two-dimensional Jander's equation in the higher temperature region.

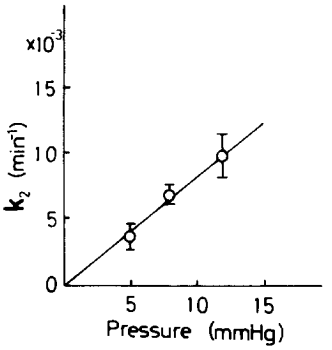

FIG. 11. Pressure dependence of rate constant k_2 of two-dimensional Jander's equation in the higher temperature region.

Arrhenius plots are made in Fig. 12 for the observed diffusion rate constants in both temperature regions. Activation energies are 15 kcal/mole in the higher temperature region and 9 kcal/mole in the lower region. These energies are used to break the bond formed at the initial stage between FeOCl and pyridine and to drive the pyridine molecule into the inner neighbor in FeOCl lattice. Thus the bonding energy between FeOCl and pyridine is smaller than these values. X-Ray diffractometry showed that the phase in the diffusion process is still a mixture of two phases—the obtained complex and pure FeOCl. This observation means that a FeOCl disk has two portions. One is the outer part of the obtained complex which has an expanded interlayer distance of 13.54 Å, and the other is the inner unreacted part of FeOCl. The edge expanded in the nucleation exerts substantial strain on the inner region of the disk. The strain weakens the bonding between the host layers. Intercalated pyridine molecules diffuse from the edge to the center, accompanying successive expansion of the interlayer distance of the inner parts. Microscopic observation showed that all crystals had fringes of the obtained complex. A similar situation was found in the case of diffusion of interlayer water in vermiculite (*8*).

Infrared spectroscopy is applied to investigate the behavior of pyridine molecules in the diffusion process. Spectra are illustrated in Fig. 13. The shaded absorptions of free pyridine in spectrum (b) are related to the vibrations of C–C in the pyridine ring, and the others in (b) are assigned to the vibrations of C–H (*9*). The absorptions of pyridine in (c), (d), and (e) are obscure because the pyridine molecules are in the host lattice. Most of the C–C vibrations of pyridine are observed in the spectra of the intercalated FeOCl, but the absorptions of C–H are much perturbed by the intercalations especially in (d) and (e). The spectrum of $FeOCl(Py)_{1/4}$ is almost the same as

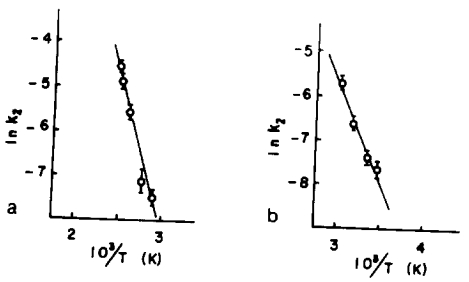

FIG. 12. Arrhenius plots for the diffusion process in the higher (a) and lower (b) temperature regions, where k_2 is the rate constant in Eq. (3).

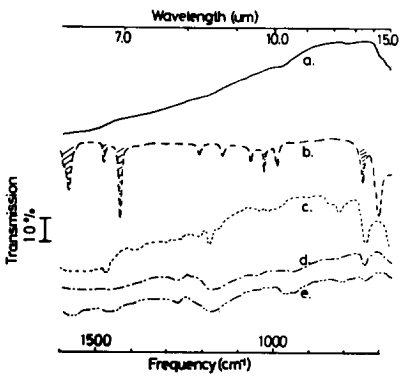

FIG. 13. Infrared spectra of FeOCl (a), pyridine (b), $FeOCl(Py)_{1/5}$ (c), $FeOCl(Py)_{1/4}$ (d), and $FeOCl(Py)_{1/3}$ (e), where $FeOCl(Py)_{1/5}$ is the process of diffusion.

that of $FeOCl(Py)_{1/3}$ except for the intensities of the absorptions, although assignments of the absorptions are not clear in this stage. Spectrum (c) has features in common with those of the free and the intercalated pyridines. Some of the intercalated pyridine molecules behave rather freely even in the diffusion process. When the intercalation is completed, all of the intercalated pyridine molecules are bound tightly to the FeOCl layer and stabilized in the interlayer region. Thus only the much perturbed spectra of pyridine are observed in (d) and (e).

In conclusion, the intercalation is understood by a nucleation followed by a diffusion. These reaction processes showed explicit two-dimensionality due to the layer structure of host FeOCl crystals. Activation energies of all processes were about 10 kcal/mole. These values are reasonable for the formation energy of the charge transfer bond between the host FeOCl and the guest pyridine molecules (*10*).

Acknowledgments

The author expresses his hearty thanks to Professor M. Koizumi of Osaka University and Professor F. Kanamaru of Okayama University for their advice and encouragement during the course of this study.

References

1. F. R. GAMBLE, F. J. DISALVO, R. A. KLEMM, AND T. H. GEBALLE, *Science* **168**, 568 (1970).
2. F. R. GAMBLE, J. H. OSIEKI, AND F. J. DISALVO, *J. Chem. Phys.* **55**, 3525 (1971).
3. G. V. SUBBA RAO AND H. W. SHAFER, *J. Phys. Chem.* **79**, 557 (1975).
4. J. V. ACRIVOS, C. DELIOS, N. Y. TOPSØE, AND J. R. SALEM, *J. Phys. Chem.* **79**, 3003 (1975).
5. S. KIKKAWA, F. KANAMARU, AND M. KOIZUMI, "Reactivity of Solids," p. 725, Plenum, New York (1977); *Bull. Chem. Soc. Japan* **52**, 963 (1979).
6. J. D. HANCOCK AND J. H. SHARP, *J. Amer. Ceram. Soc.* **55**, 74 (1972).
7. C. RIEKEL AND R. SCHÖLLHORN, *Mater. Res. Bull.* **11**, 369 (1976).
8. G. F. WALKER, *Nature* **177**, 239 (1956).
9. D. COOK, *Canad. J. Chem.* **39**, 2009 (1961).
10. C. REID AND R. S. MULLIKEN, *J. Amer. Chem. Soc.* **76**, 3869 (1954).